

See discussions, stats, and author profiles for this publication at: <https://www.researchgate.net/publication/321331994>

Mathematical modeling of mature oil paint networks

Conference Paper · September 2014

CITATIONS

5

READS

201

5 authors, including:



Piet D. Iedema

University of Amsterdam

155 PUBLICATIONS 2,258 CITATIONS

[SEE PROFILE](#)



Joen J. Hermans

Rijksmuseum Amsterdam

30 PUBLICATIONS 348 CITATIONS

[SEE PROFILE](#)



Katrien Keune

Rijksmuseum Amsterdam

84 PUBLICATIONS 1,201 CITATIONS

[SEE PROFILE](#)



Annelies van Loon

Rijksmuseum Amsterdam

71 PUBLICATIONS 894 CITATIONS

[SEE PROFILE](#)

Some of the authors of this publication are also working on these related projects:



Research into Rembrandt's painting technique and materials using macro- and microscale imaging techniques [View project](#)



The Girl in the Spotlight: A technical re-examination of Vermeer's Girl with a Pearl Earring [View project](#)

Mathematical modeling of mature oil paint networks

PIET D. IEDEMA*

Van 't Hoff Institute for Molecular Sciences
University of Amsterdam
Amsterdam, The Netherlands
p.d.iedema@uva.nl

JOEN J. HERMANS

Van 't Hoff Institute for Molecular Sciences
University of Amsterdam
Amsterdam, The Netherlands

KATRIEN KEUNE

Van 't Hoff Institute for Molecular Sciences
University of Amsterdam
Amsterdam, The Netherlands

ANNELIES VAN LOON

Van 't Hoff Institute for Molecular Sciences
University of Amsterdam
Amsterdam, The Netherlands
Royal Picture Gallery Mauritshuis
The Hague, The Netherlands

MAARTJE J.N. STOLS-WITLOX

Faculty of Humanities
University of Amsterdam
Amsterdam, The Netherlands

*Author for correspondence

KEYWORDS: mathematical modeling, oil paint, degradation, networks, aging

ABSTRACT

A kinetic model was developed as a first step in constructing a mathematical model describing the structural change of an oil paint network consisting of triacylglyceride (TAG) units during long-term degradation. The kinetic model describes the drying stage of linseed oil in terms of the functional groups partially reacting to cross-links from rate coefficients of around 70 reactions. Validation of the model was performed with experimental data on total peroxide content (peroxide value, PV) and oxygen uptake. The occurrence of a maximum in the PV and other trends are correctly predicted, including the accelerated drying effect of metal-ion based drying agents. After future implementation of hydrolysis reactions and longer-term degradation effects, the kinetic model should be able to predict the connectivity of TAG units in oil paint networks. This model will allow the construction of the network topology model.

INTRODUCTION

The objective of the mathematical model is to describe quantitatively the microstructure of the three-dimensional polymeric network of a mature oil paint system. The construction of such a comprehensive mathematical model is new to the field of conservation. Earlier publications have contributed to an overview of reactions involved in the drying and aging stage of the oil, at shorter and longer time scales (Hubert et al. 1997, Mallégo et al. 2000, Van den Berg 2002, Van Gorkum and Bouwman 2005, Soucek et al. 2012). The curing of oil paint is a complex process where bond-forming reactions, pigment-oil interactions, and degradation reactions compete with each other. However, until now most descriptions have been mainly of a qualitative nature.

This paper describes the first stage of the modeling activities in the PAInT project (Van Loon et al. 2012): the construction of a kinetic model. The most important reactions of the unsaturated moieties and functional groups in the triacylglycerides (TAGs) during drying and aging of linseed oil paint are incorporated and quantified in this model. The model's inputs consist of the initial concentrations of all compounds involved and the kinetic rate coefficients. As output, the model generates concentration profiles of these compounds and their reaction products. It also provides information concerning cross-links, which form the basis for the second stage of the modeling: network formation.

It is known that curing linseed oil is a system of complex (radical) reactions involving many compounds and reaction steps. Since only few of the reactions have been studied individually, this attempt to describe the whole system in a quantitatively correct manner is a challenging task. This effort is motivated by the expected result: a significantly improved quantitative understanding of the drying, aging, and degradation of oil paints, including the effects of different pigments and the influence of temperature, light and/or relative humidity, and the possibility to predict the influence of conservation treatments on the degradation of oil paint.

This paper is structured as follows. First, the authors will introduce the overall modeling approach leading to a quantitative understanding of network formation. Then, the main focus will be kinetic modeling, giving a description of the curing reactions involved. Subsequently, a strategy to validate the

model will be presented with experimental data from the literature, mainly on the peroxide value and oxygen consumption. In addition, the first results will be shown and compared to experimental drying data.

COMPUTATIONAL PROCEDURES

Overall objective: understanding and quantifying network formation

A polymeric approach is used, which means that the network is described in terms of its *topology*: the connectivity between the cross-links of the network and the numbers of “units” between them. This is similar to the way monomer units are connected in a branched polymer molecule or polymer network. The units of the network are the TAGs, esters of glycerol with long-chain fatty acids with one or more unsaturated bonds. They may become connected by cross-links that are formed by hydrogen abstraction or by addition reactions at the unsaturated bonds. Thus, at the start of the curing process, two fatty acids of two different non-cross-linked TAGs may become cross-linked by “consuming” the unsaturations and a network of two units is created. Subsequently, at a remaining double bond, a third TAG may become connected, and so on. The chosen modeling technique is based on Monte Carlo simulations, meaning that all the cross-linking and other events occur with a previously calculated probability. This technique has been applied before to branch formation and chain scission of polymers (Iedema et al. 2004), with or without network formation (Tobita and Hamielec 1992, Dušek 2007). Note that modeling of the network topology is not dealt with in the present paper.

Kinetic model

The probability of units becoming connected or chains undergoing scission is calculated using the *kinetic model*, which is the topic of this paper. It consists of the main kinetic rate equations describing cross-linking in competition with chain scission. The rate equations are in the form of ordinary differential equations (ODE):

$$\frac{dS}{dt} = \underbrace{\sum_i k_{pS,i} A_i^{a_i} B_i^{b_i}}_{\text{production terms}} - \underbrace{S^s \sum_j k_{cS,j} C_j^{c_j}}_{\text{consumption terms}} \quad (1)$$

This indicates that species S is produced by a number of reactions, i from components A_i and (eventually) B_i with a rate constant $k_{pS,i}$, while in similar notation it is consumed by reactions, j , with components C_j and rate coefficient $k_{cS,j}$. S , A_i and B_i denote the molar concentrations (kmole/m^3). The superscripts refer to the order in which the component is involved in the reaction; in this case, they mostly equal one. Obviously, some species are only produced or consumed. As many ODEs may be constructed as there are species. If the set of ODE equations is constructed in a consistent manner, taking all production and consumption terms of all species into account, the mass of the components is conserved. For the present model, a set of 70 ODEs was implemented in MATLAB and the system was solved using the standard ODE subroutine “ode15s.m.”

In the kinetic model, the reactions of *functional groups* are described rather than complete molecules (see Figure 1). Thus, S , A_i and B_i refer to the molar

concentrations of the groups. These groups represent fatty acid chain segments consisting of several constituents that react chemically as one system, mainly due to the presence or creation of conjugated double bonds. The groups are chosen so that their reactions proceed independently from other groups inside the same (cross-linked) molecule. The format of this paper allows only a few of the most important reaction steps that have been collected from the literature (Van den Berg 2002, Van Gorkum and Bouwman 2005, Soucek et al. 2012) and implemented in the kinetic model to be described.

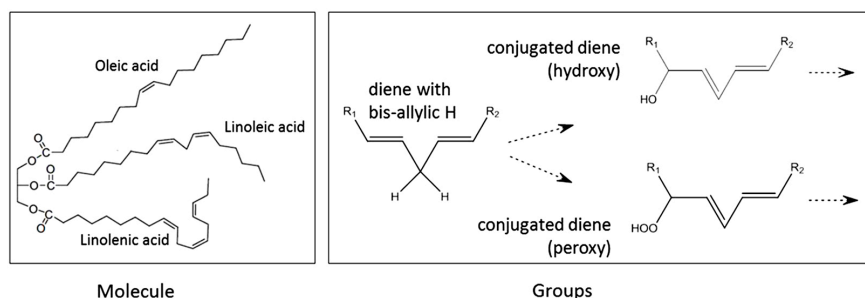


Figure 1

Model representation of molecule and groups. The diene group with bis-allylic H represents a system of two double bonds surrounding a CH_2 -group in between an R_1 and R_2 group as part of one linoleic or linolenic acid tail. The R_1 and R_2 form the remainder of the molecule, one the part of the tail connected to the two other fatty acid tails (eventually to other molecules via cross-links), and the other to the smaller part of the tail (also possibly cross-linked). In the conjugated dienes shown, one H is substituted by a hydroxy or a hydroperoxy group. The dienes may undergo further reactions

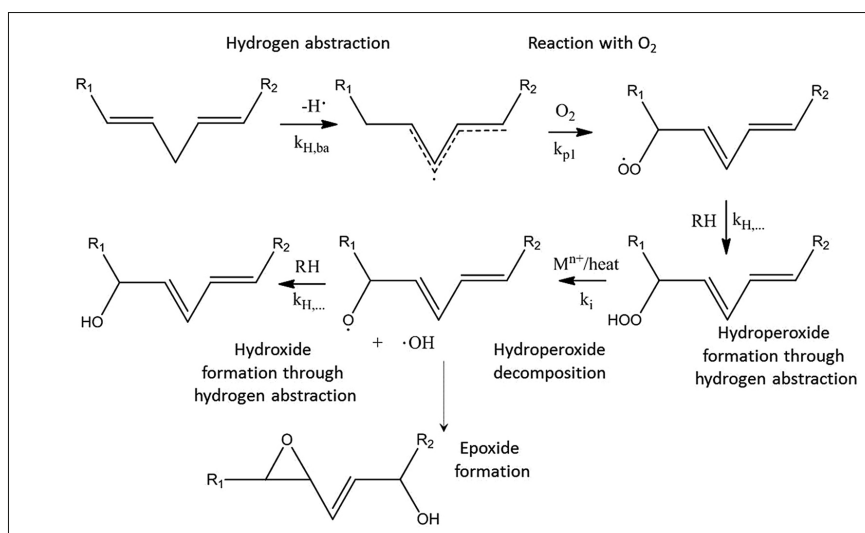


Figure 2

A sequence of reaction steps starting at a bis-allylic diene group. After hydrogen abstraction, several propagation steps lead to a hydroxide group. All the radical species may undergo termination by recombination leading to cross-links. Alternatively, the $\text{O}\cdot$ radical group may undergo beta scission or, after a series of steps, react into an epoxide group

The first step in what is commonly denoted as the ‘drying’ of an oil paint is *initiation*, the decomposition of an unstable compound under the influence of UV light or heat, yielding radicals. This is followed by *propagation* steps. A very important reaction here is hydrogen abstraction – the first step in Figure 2. In particular, the so-called “bis-allyl hydrogen” (see Figure 1) is easily removed to produce a secondary radical site. This hydrogen is available in some of the non-conjugated tails of the TAGs in linseed oil. The conjugated radical groups undergo several reactions, for instance

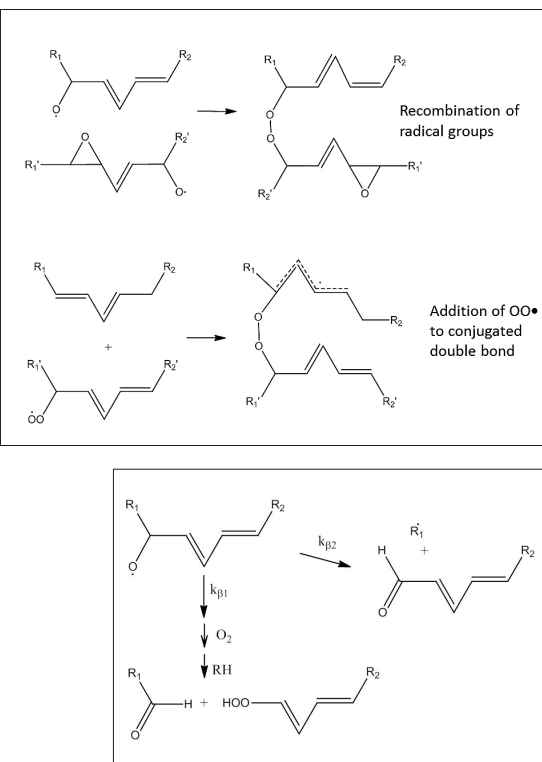


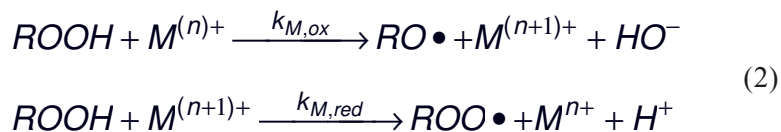
Figure 3

Formation of O-O cross-links by recombination of two $O\bullet$ radical groups (top) and by an addition reaction between a group containing $OO\bullet$ and a conjugated diene group (bottom). The addition step is followed by a termination by a disproportionation reaction with another radical group

Figure 4

Beta scission of conjugated diene group with $O\bullet$. Both scission schemes lead to (intermediate) radical species that undergo the usual radical reactions. Note that the scission reaction in both cases leads to splitting up of the molecule in two parts, one containing R_1 and the other R_2

with oxygen to form peroxide radical groups (step 2) which, among other reactions, may abstract hydrogen to turn into hydro peroxide groups (step 3). These groups may undergo homolytic decomposition yielding hydroxyl radical groups. This step is strongly catalyzed by transition metal ions. The accelerated drying of linseed oil films in the presence of such ions is thought to proceed according to:



The hydroxyl radical groups may undergo beta scission (see below) or, by hydrogen abstraction, end up as conjugated dienes (last step).

The sequence of radical reactions comes to an end when one radical group reacts with another in a *termination* step. Since many radical species exist, a multitude of such reactions occurs. Recombination reactions lead to RR , ROR , and $ROOR$ cross-links (see Figure 3). Conjugated diene groups undergo hydrogen abstraction less easily, but may participate in addition reactions leading to $ROOR$ cross-links (Figure 3). These propagation reactions lead to the formation of radical-containing groups, which subsequently undergo another type of termination reaction: disproportionation. Via these reactions between two radical groups, the radicals on both disappear.

Another important reaction is *beta scission* of groups containing an $O\bullet$ radical. The reaction may proceed according to two schemes, as shown in Figure 4. In both schemes, radicals are formed that participate in all radical reactions, and the reaction is therefore usually considered as an important phenomenon in the oil drying process. At the same time, beta scission leads to a decomposition of the oil network, since the connection between the parts of the molecules containing R_1 and R_2 is broken. The scission reactions seem to be most responsible for the emission of small and volatile organic compounds: alcohols, aldehydes, and acids.

Apart from the usual initiation–propagation–termination reactions, a number of other reactions were implemented, like the formation of an epoxide group from an $O\bullet$ radical group (Figure 2). The unstable epoxide may undergo a ring opening reaction and the resulting radical groups may again participate in all the reactions. Furthermore, reactions with antioxidants – radical scavenging reactions both with initiator radicals and conjugated radical groups (Figure 2) – were implemented that may delay the curing process.

Finally, the possibility of limited oxygen diffusion, which may cause partial oxygen depletion in the case of thicker films or fast drying (drier enhanced), was accounted for. A simple model to describe the oxygen concentration in the film, $[O_2]$, was employed:

$$\frac{d[O_2]}{dt} = k_{m,O_2}([O_2]^* - [O_2]) - [O_2] \sum_i k_{i,O_2} c_{i,\bullet} \quad (3)$$

Here, k_{m,O_2} is the mass transfer rate, $[O_2]^*$ the saturation concentration in the film, and $c_{i,\bullet}$ the concentration of the diene radical group, which react with oxygen at the coefficient rate k_{i,O_2} .

Regarding this complex set of reactions and transport phenomena, a number of *a priori* assumptions are unavoidable at this stage of modeling:

- Bis-allyl H groups undergo hydrogen abstraction at a higher rate than conjugated dienes.
- For reasons of steric hindrance at each group, a maximum of two cross-links may be created; further substitutions lead to hydroxide or epoxide.
- All radical groups participate in hydrogen abstraction.
- Only $\text{OO}\cdot$ radical groups induce addition reactions with conjugated double bonds.
- Hydro peroxides decompose faster than peroxide cross-links (ROOR).

The present version of the kinetic model only contains the reactions described above; hence its use is limited to the drying stage of an oil paint layer – in the order of months for linseed oil. Hydrolysis and longer-term degradation effects, for instance by further radical reactions, or further metal ion catalyzed reactions resulting from pigment-oil interactions, are not yet accounted for in the model.

Model strategy

Seventy of the most relevant initiation, propagation, termination, and other reactions involved in linseed oil curing were compiled from the literature. This led to a set of 70 ODEs and an even higher number of rate coefficients. Virtually none of these coefficients are available from the open literature. This forces us to infer coefficients in an indirect manner from experimental data on measured quantities. Various data are available, such as IR spectra measured at different drying stages, quantities of small organic compounds evolving during drying, oxygen consumption, and the “peroxide value” (PV). The latter is a measure of the overall content of peroxy groups, both ROOH and ROOR . In principle, all the measured concentrations or amounts of species present are accessible from the model. However, until now, the authors have limited themselves to using a PV and oxygen consumption profile over time from Mallégol et al. (2000) and Oymans et al. (2005). Both are usually seen as important indicators of the progress of drying of oil films.

RESULTS AND DISCUSSION

Model validation

The major kinetic mechanisms governing the PV and oxygen profile and the values of the corresponding kinetic rate coefficients are not known. By varying all of the coefficients in the model so as to obtain a best fit for the experimental PV and oxygen profiles, the major mechanisms and coefficients are identified. The PV profile from the model was compared to the experimental data from Mallégol et al. (2000), both in the absence and presence of a metal-based drier. The values of the rate coefficients were varied to achieve the best agreement in terms of the *time* instant of the maximum PV value and the *level* of that maximum. The results are shown

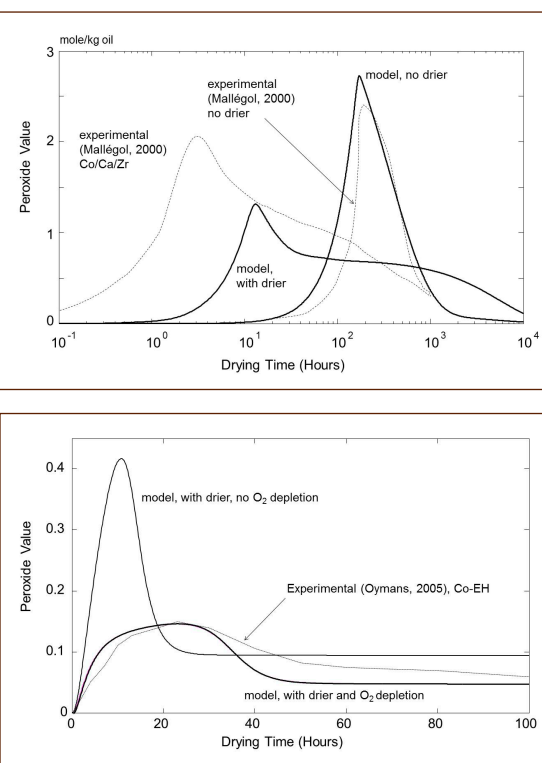


Figure 5

PV profile on a logarithmic time scale, both simulated and experimental (Mallégol et al. 2000), with and without drying agent. The drying agent is a mixture of cobalt ethylhexanoate and calcium and zirconium octoates (Co/Ca/Zr)

Figure 6

Comparison of PV profiles for a case with a drier with experimental PV data from Oymans et al. (2005). A better agreement is obtained if oxygen depletion is accounted for in the model. The drying agent is cobalt ethylhexanoate (Co-EH)

in Figure 5. The rate coefficients obtained from this tuning operation are listed in Table 1, together with a number of other simulation variables.

Table 1

Kinetic rate coefficients and other key variables

Rate Coefficient	Value	Unity
Initiation	$5 \cdot 10^{-5}$	s^{-1}
Hydrogen abstraction, bis-allyl H	10	$m^3 kmole^{-1} s^{-1}$
Hydrogen abstraction, conjugated =	0.8	$m^3 kmole^{-1} s^{-1}$
Hydrogen abstraction, conjugated = OH	0.8	$m^3 kmole^{-1} s^{-1}$
HA by $O\bullet$ and $OO\bullet$, bis-allyl	8	$m^3 kmole^{-1} s^{-1}$
Recombination termination	1200	$m^3 kmole^{-1} s^{-1}$
Disproportionation termination	1200	$m^3 kmole^{-1} s^{-1}$
Propagation with O_2	313	$m^3 kmole^{-1} s^{-1}$
Hydroperoxide (ROOH) decomposition	$8 \cdot 10^{-7}$	s^{-1}
Peroxy (ROOR) decomposition	$5 \cdot 10^{-8}$	s^{-1}
Beta scission (type 1)	0.01	s^{-1}
Drier metal oxidation, $k_{M,ox}$	$5 \cdot 10^{-3 \ 1)}, 10^{-2 \ 2)}$	$m^3 kmole^{-1} s^{-1}$
Drier metal reduction, $k_{M,red}$	$7.1 \cdot 10^{-5 \ 1)}, 1 \ 2)$	$m^3 kmole^{-1} s^{-1}$
O_2 mass transfer coefficient, k_{m,O_2}	0.05	s^{-1}
Concentrations		
Initial concentration bis-allyl H	3.9	$kmole \ m^{-3}$
Equilibrium oxygen concentration, $[O_2]^*$	$8 \cdot 10^{-4 \ 3)}$	$kmole \ m^{-3}$
Initial oxygen concentration, $[O_2]$	$4 \cdot 10^{-4 \ 3)}$	$kmole \ m^{-3}$
Initial metal ion concentration, $[M^{n+}]$	$0.15 \ 1), 0.012 \ 2)$	$kmole \ m^{-3}$

1) In comparison with Mallégol et al. (2000)

2) In comparison with Oymans et al. (2005)

3) From Parenti et al. (2007)

Comparison of kinetic model outcomes with experimental data

Figure 5 shows the PV profile on a logarithmic time scale as calculated from the model for cases with and without a drier together with two experimental profiles from Mallégol et al. (2000), obtained with paint layer samples of $20 \mu m$. In the case without a drier, good agreement is seen. In the case with a drier, the PV trend is well predicted by the model, a maximum followed by a slow decay. However, the model shows less drying time reduction and a lower PV maximum. Simulations reveal that, by adding a drier, the drying acceleration and the lowering of the PV maximum are inseparable effects. Note that the completely different shapes of the PV profiles from the model are caused solely by the presence or absence of metal ions.

The calculated PV profiles were compared, using the same kinetic data as before, with another set of experimental oil curing data from Oymans (2005) for a linseed oil film of 1 mm thickness in an open Petri dish using cobalt-ethylhexanoate (Co-EH) as a drier. The result is shown in Figure 6. Assuming no oxygen mass transfer limitation and hence no depletion, the maximum PV level was found to be much higher than the experimentally observed one. In view of the layer thickness, O_2 depletion might be an important effect in this case. Taking limited O_2 diffusion into account, the model shows good agreement with the experimental data.

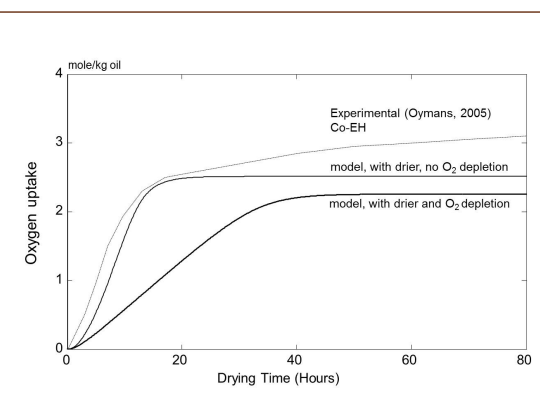


Figure 7

Comparison of cumulative oxygen uptake from model and experimental O_2 data (Oymans et al. 2005). Here, a better agreement is achieved if no transport limitation for oxygen is assumed

The cumulative oxygen uptake as calculated by the model was also compared to data reported by Oymans et al. (2005) obtained using the same chemicals, but a different experimental setup – a closed flask. In Figure 7, the model results are compared to these data. Applying exactly the same conditions as those yielding the best fit for the PV profile, a slower O_2 uptake profile than measured is observed. This would suggest that there is no transport limitation effect for oxygen in this case. Indeed, in the absence of O_2 depletion, a very good fit is obtained.

Based on the validated model discussed above, a number of observations, both general and with respect to specific kinetic mechanisms, can be listed:

- The drying process occurs in two stages. At first, a fast process is observed in which the bis-allyl H concentration drops to zero and the peroxide concentration (PV value) reaches a maximum. Then, in a slower process, the PV decreases. Initiator radicals act as a “seed” to the curing process; neither the quantity of the initiator source nor the initiator decomposition rate coefficient influences the PV and O_2 profile; there is no role for antioxidants.
- The PV and O_2 profile is very sensitive to the rate coefficients of hydrogen abstraction and oxidation (steps 1 and 2 in Figure 2).
- The rate of hydro peroxide decomposition is crucial for the drying time; the accelerating effect of metal ions through the reaction scheme (2) is clearly observed.
- Beta scission and cross-linking by addition (Figure 3) seem to be of minor effect.
- Epoxide formation does not influence the PV and O_2 profile.
- Antioxidants reacting with a conjugated radical group delay the start-up of the drying process; however, the experimental data do not reveal clear delaying by inhibition.

These are the main conclusions concerning the rate coefficients for the PV and O_2 profile only. Further fine-tuning of the model with other data is required to account for effects on other experimentally observed phenomena. For simulations of the PV and O_2 profile, the rate coefficients of the non-important mechanisms, including inhibition, have been set equal to zero.

CONCLUSION

As a first stage in the construction of a comprehensive model to predict the structure of a linseed-oil-based network, a kinetic model containing all the relevant reactions for the curing process was developed. The model consists of the rate equations in terms of the concentration of functional groups based on the reactivity of conjugated parts of fatty acid chains. Until now, the model has been validated with experimental data by Mallégol et al. (2000) and Oymans et al. (2005), concerning the time profiles of peroxide value and the oxygen uptake. Model simulations clearly demonstrated the importance of the hydrogen abstraction of the bis-allyl H group and the subsequent reaction with oxygen. Cross-linking by addition reactions between $OO\bullet$ and conjugated double bonds and inhibition reactions appeared

to play a minor role. The experimentally observed maximum in the PV is clearly reproduced by the model. The strong acceleration of the drying process by adding drying agent is correctly predicted by the model. Some of the differences in the level of the PV maximum could be explained by oxygen transport limitation. Good agreement was obtained for the initial stage of the oxygen uptake. The issue of oxygen depletion has not been explicitly explored by experiment. If this phenomenon turns out to be important, even in thin oil paint films, new drying experiments have to be conducted, closely mimicking conditions in drying oil films.

The authors conclude that the kinetic model as validated with the PV and oxygen profile forms an important first step toward a complete quantitative description of the complex curing process. It will then be possible to translate the model results, in terms of conversion and cross-linking of groups, to those quantities in complete TAG molecules. Ultimately, this will form the basis of the Monte Carlo network simulation with the cross-linked TAG molecules as the building blocks.

REFERENCES

- DUŠEK, K.** 2007. My fifty years with polymer gels and networks and beyond. *Polymer Bulletin* 58: 321–338.
- HUBERT, J.C., R.A.M. VENDERBOSCH, W.J. MUIZEBELT, R.P. KLAASEN, and K.H. ZABEL.** 1997. Mechanistic study of drying of alkyd resins using (Z,Z)- and (E,E)-3,6-nonadiene as model substances. *Progress in Organic Coatings* 31: 331–340.
- IEDEMA, P.D. and H.C.J. HOEFSLOOT.** 2004. Predicting branched architectures from molecular weight and degree of branching distribution of polyethylene for single and mixed systems with a constrained geometry metallocene catalyst in continuous reactors. *Polymer* 17: 6071–6082.
- MALLÉGOL, J., J. LEMAIRE, and J.-L. GARDETTE.** 2000. Drier influence on the curing of linseed oil. *Progress in Organic Coatings* 39: 107–113.
- OYMANS, Z.O., W. MING, and R. VAN DER LINDE.** 2005. Oxidation of drying oils containing non-conjugated and conjugated double bonds catalyzed by a cobalt catalyst. *Progress in Organic Coatings* 54: 198–204.
- PARENTI, A., P. SPUGNOLI, P. MASELLA, and L. CALAMAI.** 2007. Influence of the extraction process on dissolved oxygen in olive oil. *European Journal of Lipid Science and Technology* 109: 1180–1185.
- SOUCEK, M.D., T. KHATTAB, and J. WU.** 2012. Review of autoxidation and driers. *Progress in Organic Coatings* 73: 435–454.
- TOBITA, H. and A.E. HAMIELEC.** 1992. Control of network structure in free-radical cross-linking copolymerization. *Polymer* 32: 3647–3657.
- VAN DEN BERG, J.D.J.** 2002. PhD dissertation, University of Amsterdam, Molart Series (6), Amsterdam: AMOLF.
- VAN GORKUM, R. and E. BOUWMAN.** 2005. Alkyd paint and paint driers. *Coordination Chemistry Reviews* 249: 1709.
- VAN LOON, A., K. KEUNE, M.J.N. STOLS-WITLOX, and P.D. IEDEMA.** 2012. PAinT – Paint alterations in time. <http://www.s4a-paint.uva.nl/>.

How to cite this article:

Iedema, P.D., J.J. Hermans, K. Keune, A. van Loon, and M.J.N. Stols-Witlox. 2014. Mathematical modeling of mature oil paint networks. In *ICOM-CC 17th Triennial Conference Preprints, Melbourne, 15–19 September 2014*, ed. J. Bridgland, art. 1604, 8 pp. Paris: International Council of Museums. (ISBN 978-92-9012-410-8)